J Solid State Electrochem (2010) 14:1051–1056
DOI 10.1007/s10008-009-0919-x

ORIGINAL PAPER

A two-step method combining electrodepositing and spin-coating for solar cell processing

Weili Yu · Bin Xu · Qingfeng Dong · Yinhua Zhou · Junhu Zhang · Wenjing Tian · Bai Yang

Received: 1 July 2009 / Revised: 30 July 2009 / Accepted: 4 August 2009 / Published online: 20 August 2009

Abstract Electrochemistry provides a simple and promising method for preparing organic solar cells (OSCs). In this paper, we present a two-step solution-based method to prepare bilayer heterojunction OSCs by electrodepositing polythiophene (PTh) and then spin-coating chloroform solution of [6,6]-phenyl C61-butyric acid methyl ester (PCBM) onto the PTh layer. The influence of film thickness on performance of bilayer solar cells was investigated, and the best performance was achieved when the thickness of PTh and PCBM was 15 nm and 30 nm, respectively. The optimized solar cell showed power conversion efficiency of 0.1% under the illumination of AM 1.5 (100 mW cm^{-2}) simulated solar light. This solution-based method offers a new way for processing bilayer OSCs.

Keywords Electrodeposition · Organic solar cells · Polythiophene · Spin coating

Introduction

In recent years, solar cells have attracted much interest because they represent an inexhaustible, clean energy source that could meet the increasing demand for energy and potentially reduce dependence on fossil fuels [1–3]. Among the various kinds of solar cells, organic solar cells (OSCs) have the merits of low cost, high flexibility, and of being amenable to high throughput roll-to-roll fabrication [4, 5]. The processing methods of OSCs are mainly focused on two ways: the spin-coating method and the vacuum evaporation deposition method, which are dedicated to polymer-based bulk-heterojunction solar cells and small-molecule-based heterojunction solar cells, respectively [6, 7].

Besides the two methods mentioned above, electrochemical deposition (electrodeposition) is another promising method which could be used to prepare solar cells. This method combines the synthesis and deposition of conducting polymer in one step, and provides a simple, fast and low-cost way for processing films and devices, such as photoelectronics, actuators, sensors, etc. [8–10]. Efforts have been made to improve solar cell performance utilizing electrochemical methods. For instance, Hümmelgen group reported single-layer devices based on electrodeposited polybithiophene and poly(3-methylthiophene) [11, 12]; Shi group reported a bulk heterojunction device by electrochemical codepositing polythiophene (PTh) and C60 simultaneously in solution [13].

Very recently, solar cells with power conversion efficiency (PCE) of nearly 1% were reported by Armstrong group using electrochemical method. The solar cells are prepared by a process which combines electrodepositing PTh and then evaporation depositing C60 on electrodeposited PTh in vacuum together [14]. Inspired by these works and to make full use of the advantages afforded by electrochemical methods, here, we present a novel way to prepare OSCs. This process combines electrochemical deposition and spin-coating method together and offers a promising way to improve performance of electrodeposited solar cells. Briefly, a thin PTh film is electrodeposited on indium-tin-oxide (ITO) glass, followed by spin-coating [6,6]-phenyl C61-butyric acid methyl ester (PCBM) solu-

W. Yu · B. Xu · Q. Dong · Y. Zhou · J. Zhang (✉) · W. Tian · B. Yang
State Key Laboratory of Supramolecular Structure and Materials, College of Chemistry, Jilin University, Changchun 130012, People's Republic of China
e-mail: zjh@jlu.edu.cn

W. Tian
e-mail: wjtian@jlu.edu.cn

tion in chloroform onto the PTh film. PTh is used as donor material due to following advantages: First, PTh has high hole mobility. Second, PTh is highly electroactive and can easily be prepared by electrochemical methods. Third, PTh is insoluble in most organic solvents which allow organic solution processing on it. The bilayer heterojunction device has a structure of ITO/PTh/PCBM/LiF/Al, and its performance was investigated by managing the electrochemical and spin-coating parameters.

Experimental details

Tetrabutylammonium hexafluorophosphate ($TBAPF_6$), thiophene, 3-thiophene acetic acid (3-TAA), and PCBM were all purchased from Aldrich and used as received without further purification. The electrochemical deposition was performed in a three-electrode system. The working electrode was ITO glass (20 Ω/square); the counter electrode was a Pt wire electrode, and the reference electrode was Ag/Ag^+ electrode. The electrolyte was 0.1 M $TBAPF_6$ in acetonitrile. The concentration of thiophene monomer is 0.1 M.

The OSCs were prepared by a two-step process. Before electrodeposition, the ITO glass was initially cleaned by detergent solution, followed by ultrasonic cleaning consequently in solutions of ethanol, acetone, and deionized water for 10 min each. After that, the ITO glass was immersed into HI solution (45 wt%) for 10 s to activate the ITO layer. Then, the activated ITO glass was rinsed with ethanol and dried under a stream of nitrogen. Next, the ITO glass was dipped in 3-TAA solution in acetonitrile (10 mM) immediately and stored for 3 h [15, 16].

As the potentiostatic deposition method could provide a smooth film at relatively high speed [17], constant potentials were employed here. In detail, a potential of 1.4 V was applied to the ITO glass for 0.5 s, then the potential was changed to 1.35 V, and the remaining time relied on the total quantity of charge passing through the cell, which reflected the thickness of PTh film. After that, the resulting PTh film was dedoped under a potential of 0.2 V for 20 s.

After electrodeposition, the PTh film was rinsed with acetonitrile and dried by nitrogen. Then PCBM solution in chloroform (7.5 mg ml^{-1}) was spin cast on the PTh film. During the spin-coating process, the acceleration and spin coating time were fixed at 200 rpm s^{-1} and 30 s, respectively, and the spin-coating speed was chosen according to the desired thickness. The PCBM solution was stirred by magnetic power for 12 h before use. For devices preparation, LiF (~0.7 nm), and Al (~70 nm) were deposited in turn under high vacuum (5×10^{-4} Pa). The active device area was 0.05 cm^2.

The electrochemical experiment was performed in an Electrochemical Station (BS100 cell stand, Bioanalytical System Inc.). UV-Visible absorption spectra were recorded on a UV-3600 spectrometer (Shimadzu). The morphology and root mean square (RMS) roughness were obtained from atomic force microscopy (AFM) height images, and AFM measurements were performed on an SPA300HV system (Seiko Instruments Inc.). The thickness of the PTh films was determined using a Dektak150 Surface Profiler (Veeco). Current density voltage (*J–V*) measurement of the devices was conducted on a computer-controlled Keithley 2400 source meter measurement system. Air Mass 1.5 global (AM 1.5) 100 mW cm^{-2} illumination from a Sciencetech 500-W solar simulator acted as a light source. All the measurements were performed under ambient atmosphere at room temperature.

Results and discussion

To be used as a donor material in solar cells, the regularity, uniformity, and film thickness of electrodeposited PTh are key parameters to be considered. The regularity of electropolymerized PTh is less than 70% [18]. The uniformity is closely related to the sweeping method of applied voltage. Here, the thickness and the morphology of PTh film were adjusted exactly by controlling the total amount of charge passing through the cell. In a separate experiment, the average PTh film thickness was found to increase about 100 nm when the total charge increased 40 mC cm^{-2}.

Figure 1 shows the current–time curve for the deposition and reduction of PTh film on the ITO electrode. Firstly, the oxidation potential was applied at 1.4 V to oxidize 3-TAA to form a seed layer. Then, the applied potential was switched to 1.35 V to electrodeposit thiophene monomer, and the thickness of electrodeposited film was controlled by tuning the oxidation time. In Fig. 1a, it can be observed that the current decreases at the beginning, which indicates that 3-TAA is polymerized and deposited onto the electrode surface. Then the current from oxidation of PTh keeps on increasing for 8 s till it stabilizes, indicating that PTh is deposited continuously. Figure 1b shows the reduction process of electrodeposited PTh film. The reduction was completed after 13 s.

Figure 2 shows the typical cyclic voltammogram for electrodeposited PTh film on ITO glass. The curve corresponds to the oxidation and reduction processes of the polymer with anion insertion to its oxidized (doped) state and extraction to its neutral (dedoped) state [19]. The cyclic voltammogram shows onset of the oxidation potential at 0.3 V, and a broad redox wave appears at the peak current of 0.68 V indicative of the unique crystalline region within the film and the concentration of head-to-tail

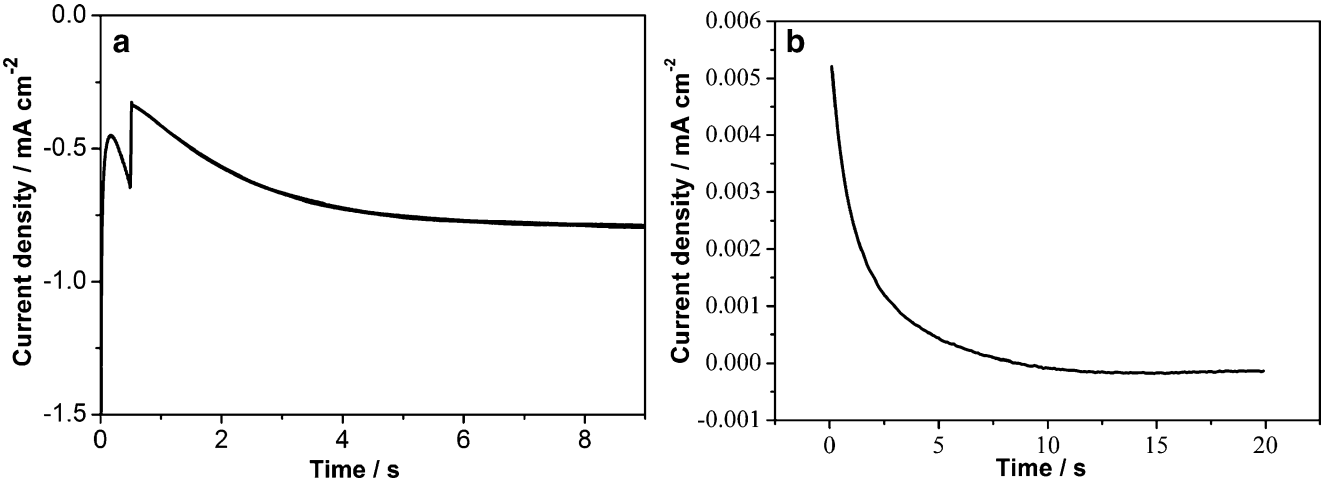

Fig. 1 Current–time profiles for electrodeopositing and dedoping PTh layer on ITO glass. **a** Oxidation potential, 1.4 V (0.5 s) and 1.35 V (9 s); **b** dedoping at 0.2 V (20 s)

coupling in this film [20]. The redox process was reversible, and no degradation occurred.

The UV-Vis absorption spectra of electrodeposited PTh before and after dedoping under 0.2 V voltage are depicted in Fig. 3. This spectra contain an absorption peak at 528 nm, which is the typical absorption of neutral state of PTh due to the π-π* transition. The absorption peak value increased after the dedoping process, which indicated that the transition from the oxidized (doped) state to the neutral (dedoped) state had occurred. The PTh energy gap value was estimated by taking the absorption onset (640 nm) to be 1.94 eV. This value was similar to that of chemically synthesized PTh, suggesting that both of them had comparable effective conjugation lengths. An isosbestic point appeared at 614 nm, suggesting a transition from the neutral state to the polaronic state existed [14].

The AFM surface morphology images of electrodeposited PTh before and after spin coating with PCBM are shown in Fig. 4. Figure 4a shows that the ITO glass is fully covered with electrodeposited PTh film which is composed of PTh protuberances with an average size of about 80 nm in diameter. It should be pointed out that to fabricate uniform thin films without pinholes, etching ITO with strong acid is necessary because it can increase the active sites of ITO glass [21]. After reaction with 3-TAA, a firm chemical bond formed between the ITO surface and 3-TAA molecules, which could enhance both surface coverage and the electron-transfer rate at the interface [14]. The polymer growth followed the two-dimensional nucleation and growth mechanism [21, 22]. The described electrodeposition process created a PTh film with average thickness of 15 nm, and the RMS value was 4.09 nm. After spin-coating with PCBM chloroform solution, the total active layer was 45 nm thick, with RMS value of 0.96 nm (Fig. 4 (b)), suggesting that the spin cast PCBM reduced the RMS value and a rough interface existed between the PTh and PCBM

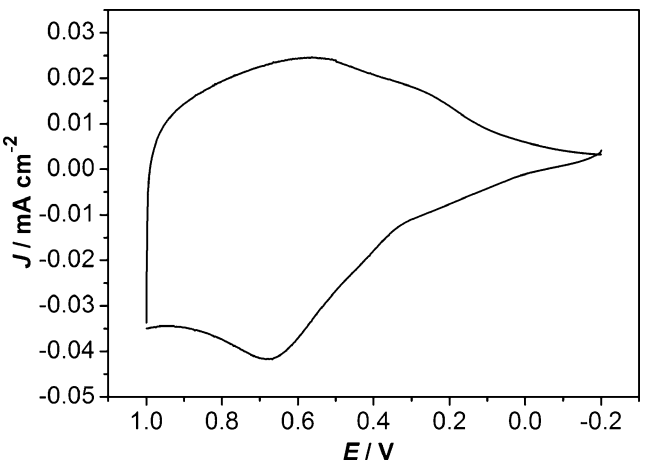

Fig. 2 Cyclic voltammogram for PTh film on ITO glass. Electrolyte, 0.1 M solution of $TBAPF_6$ in acetonitrile, scan rate 50 mV s^{-1}

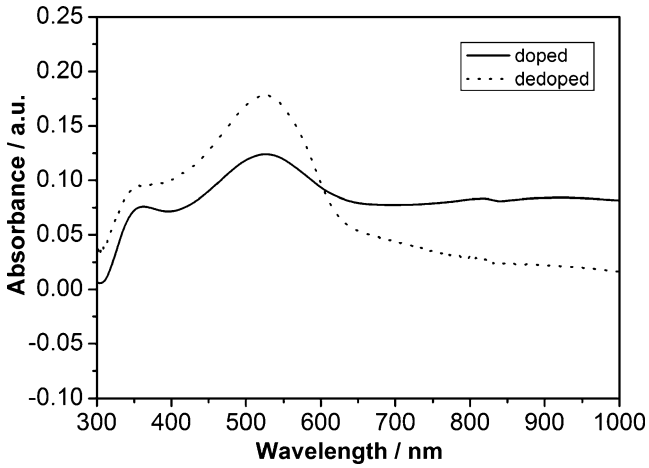

Fig. 3 The UV-Vis absorption of PTh film before and after dedoping at 0.2 V

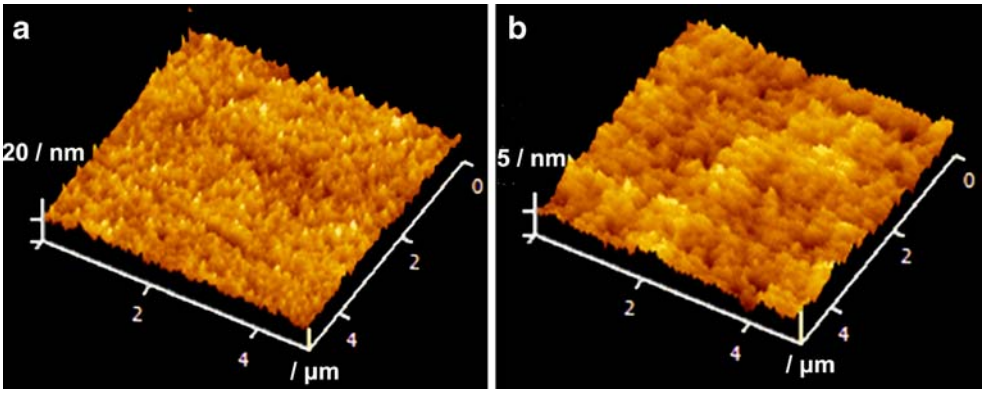

Fig. 4 The AFM images of the topography of **a** PTh film and **b** PTh film covered by PCBM layer. The scan size was 5×5 μm^2 and Z range was 20 nm and 5 nm, respectively

layers. Comparing with a planar surface, the rough interface might create a larger interface, which would produce more opportunities for excitons to separate into electrons and holes. We have also investigated chlorobenzene as a solvent instead of chloroform with the same concentration, however, no photoelectricity was observed, possibly due to the weak volatility of chlorobenzene, resulting in a much thinner PCBM layer and large leak current. The schematic structure of the solar cell is shown in Fig. 5 (left). The simulated rough PTh surface was acquired from AFM image (bottom right) and the line profile (top right). From the line profile, we can see that the height difference of the PTh surface was more than 10 nm while the thickness of PCBM was about 30 nm, suggesting that the leak current between the PTh layer and the Al cathode was blocked off by the PCBM layer.

The thickness of active layer in bilayer solar cells is key to the photovoltaic performance. A thicker active layer is better for light adsorption, however, a thicker film might result in a higher series resistance (R_s) for the device, increases the possibility of charge carrier recombination, and will reduce the short-circuit current (J_{sc}) and the fill factor (FF) [23]. So an optimum film thickness was believed to exist. The effects of the thicknesses of the PTh layer and the spin cast PCBM layer on the performance of the cells were investigated thoroughly. The thickness of the PCBM layer was mainly controlled by the PCBM concentration and the spin-coating process. In this case, the solar cell showed the best performance when the PCBM layer was 30-nm thick which was prepared by spin-coating PCBM solution in chloroform with the concentration of 7.5 mg ml^{-1} under following process (acceleration, 200 rpm s^{-1}; speed, 2,000 rpm, spin time: 30 s). The influence of PTh film thickness on J_{sc} and PCE is shown in Fig. 6a with a PCBM thickness of 30 nm. It was observed that the J_{sc} and the PCE had a peak value when the thickness of PTh was about 15 nm. The increase of PCE was mainly consistent with the changing J_{sc}, and when the PTh thickness was thinner than 25 nm, the J_{sc} was above 0.3 mA cm^{-2}. As charge carriers are mainly formed at the organic heterojunction and extracted by the built-in electric field, the increase of J_{sc} confirms that an effective bilayer heterojunction formed. Note that the J_{sc} decreases quickly when PTh is thicker than 40 nm; we suggest the increased diffusion distance for charge carriers is the main reason as the PTh is dedoped. The influence of PTh film thickness on FF and open-circuit voltage (V_{oc}) is shown in Fig. 6b. When PTh film was between 10 nm and 40 nm, the V_{oc} was stable at about 0.6 V which is believed to be decided by the difference between the highest occupied molecular orbital level of PTh and the lowest unoccupied molecular orbital level of PCBM [4]. When PTh layer was thinner than 10 nm, the V_{oc} went below 0.2 V, suggesting that there was leak current loss at the ITO/PTh interface [24]. When the PTh layer was thicker than 40 nm, the V_{oc} was large even up to 0.8 V, which was a typical

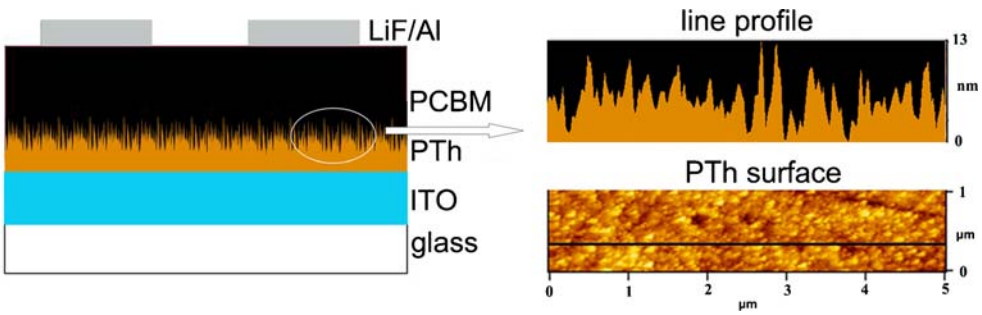

Fig. 5 The schematic structure of the solar cell (*left*) and AFM image (*bottom right*) of PTh/PCBM intersurface with profile line (*top right*)

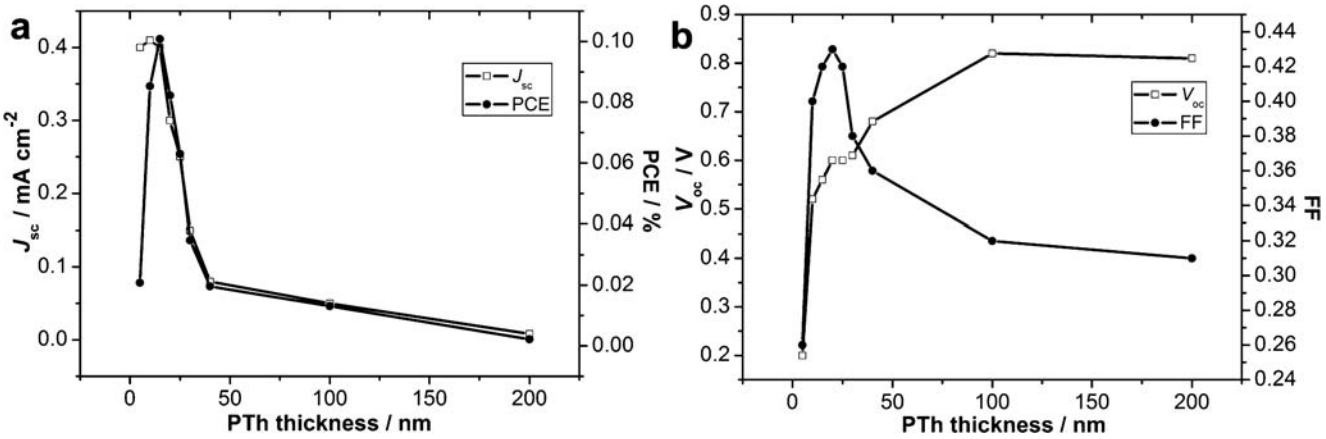

Fig. 6 **a** Influence of PTh film thickness on the short-circuit current density (J_{sc}) and power conversion efficiency (PCE); **b** Influence of PTh film thickness on fill factor (FF) and open-circuit voltage (V_{oc}) of solar cells. For all devices, the PCBM layer is 30-nm thick

characteristic of single-layer devices. The FF was mainly between 0.32 and 0.43. This reason might lie in R_s. As FF is a function of R_s and exciton drift length (L_d), in this case, R_s (calculated by the slope reciprocal of the *J-V* curves at J=0 [25]) is typically above 250 Ω cm^2 which is about 30 times magnitude of R_s in typical spin-cast OSCs [6]. This might also explain the relative lower J_{sc} value. According to previous reports, the L_d of electrodeposited conjugated polymer is usually in the range of 5 nm to 20 nm [26, 27]. This result is in accordance with the PTh thickness in our bilayer device.

The *J-V* curves of the optimized solar cell of ITO/PTh (15 nm)/PCBM (30 nm)/LiF/Al in the dark and under AM 1.5 (100 mW cm^{-2}) illumination are shown in Fig. 7. For comparison, a single PTh layer device with structure of ITO/PTh (75 nm)/LiF/Al was also presented. Note that the PTh thickness in the single-layer device is much thicker than that of bilayer device [7, 26]; it is believed that a thicker film is necessary to reduce the leak current caused by rough morphology. The *J-V* characteristics of these two devices under illumination of AM 1.5 (100 mW cm^{-2}) were summarized in Table 1. Comparing with the single-layer device, it's clear that the PCE was greatly enhanced after spin coating the PCBM layer from 0.004% to 0.1%. The J_{sc} was 25 times higher than that of the PTh single-layer device, although the V_{oc} was slightly decreased from 0.8 V to 0.6 V. This result confirmed that after spin-coating PCBM, an effective bilayer heterojunction was formed between the PTh layer and the PCBM layer, resulting in improved exciton dissociation and charge generation at the PTh/PCBM interface. After spin coating the PCBM layer, the FF increased from 0.26 to 0.42, which was in accordance with the decreasing in R_s from above 10 kΩ cm^2 to 269 Ω cm^2. This experiment indicated that the spin-coating PCBM was able to amend the rough surface and improve the extraction of the charge carriers generated between electrodeposited PTh and the PCBM layer. It is worth mentioning that the PCE of 0.1% is much lower than bulk heterojunction solar cell processed by the spin coating process, however, it is a step forward for improving the feasibility of processing OSCs by electrochemical techniques. What's more, as PTh can be electrodeposited on the electrode directly, utilizing lithography techniques or patterned electrodes, it is possible to fabricate ideal devices with nano scale phase separation to enlarge the interface area and enhance the PCE further.

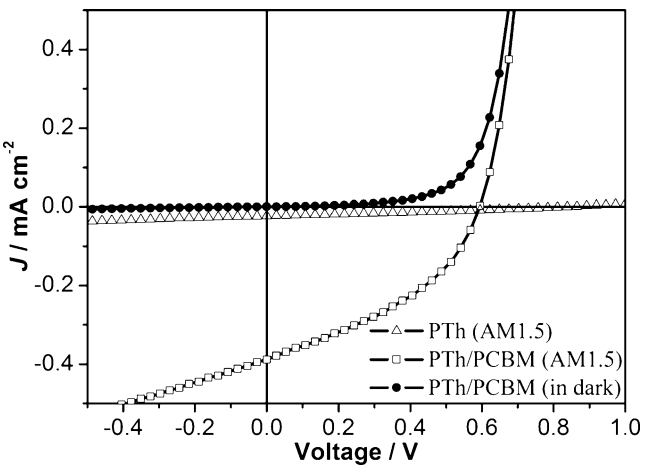

Fig. 7 Current density–voltage (*J–V*) characteristics of PTh/PCBM bilayer device in dark and under AM 1.5 illumination (100 mW cm^{-2}). For comparison, PTh single layer device was also presented

Table 1 The performances of single-layer (PTh) and bilayer (PTh/PCBM) solar cell devices under illumination of AM 1.5 (100 mW cm^{-2})

Active layer	J_{sc}/mA cm^{-2}	V_{oc}/V	FF	PCE/ %
PTh	0.02	0.8	0.26	0.004
PTh/PCBM	0.4	0.6	0.42	0.1

Conclusions

We constructed a bilayer solar cell by a two-step process which combined electrodepositing PTh in acetonitrile solution and spin coating PCBM from chloroform together. The influence of PTh thickness on solar cell performance was investigated. The performance of the solar cell was greatly enhanced compared with the electrodeposited PTh single-layer device. The PCE of 0.1% under AM1.5 (100 mW cm^{-2}) was acquired when the thickness of PTh and PCBM were 15 nm and 30 nm, respectively. This bilayer heterojunction solar cell fabricated by electrodeposition and spin-coating techniques provides a new approach for the processing of large scale OSCs.

Acknowledgements This project was supported by the National Natural Science Foundation of China (No.20534040) and National Basic Research Program of China (No.2007CB936402). The authors thank Trent Johnson from West Virginia University for his help with the writing of this paper.

References

1. Tang CW (1986) Appl Phys Lett 48:183
2. Yu G, Gao J, Hummelen JC, Wudl F, Heeger AJ (1995) Science 270:1789
3. Peumans P, Uchida S, Forrest SR (2003) Nature 425:158
4. Gunes S, Neugebauer H, Sariciftci NS (2007) Chem Rev 107:1324
5. Thompson BC, Frechet JMJ (2008) Angew Chem Int Ed 47:58
6. Ma W, Yang C, Gong X, Lee K, Heeger AJ (2005) Adv Funct Mater 15:1617
7. Peumans P, Bulović V, Forrest SR (2000) Appl Phys Lett 76:2650
8. Schroeder R, Majewski LA, Grell M, Maunoury J, Gautrot J, Hodge P, Turner M (2005) Appl Phys Lett 87:113501
9. Pyo M, Bohn CC, Smela E, Reynolds JR, Brennan AB (2003) Chem Mater 15:916
10. Xue M, Zhang Y, Yang Y, Cao T (2008) Adv Mater 20:2145
11. Leguenza EL, Patyk RL, Mello RMQ, Micaroni L, Koehler M, Hümmelgen IA (2007) J Solid State Electrochem 11:577
12. Valaski R, Muchenski F, Mello RMQ, Micaroni L, Roman LS, Hümmelgen IA (2006) J Solid State Electrochem 10:24
13. Fan B, Wang P, Wang LD, Shi GQ (2006) Sol Energy Mater Sol Cells 90:3547
14. Ratcliff EL, Jenkins JL, Nebesny K, Armstrong NR (2008) Chem Mater 20:5796
15. Donley C, Dunphy D, Paine D, Carter C, Nebesny K, Lee P, Alloway D, Armstrong NR (2002) Langmuir 18:450
16. Zotti G, Schiavon G, Zecchin S (1998) Langmuir 14:1728
17. Fu M, Shi G, Chen F, Hong X (2002) Phys Chem Chem Phys 4:2685
18. Leclerc M, Diaz FM, Wegner G (1989) Macromol Chem Phys 190:3105
19. Yassar A, Roncali J, Garnier F (1989) Macromolecules 22:804
20. Skompska M, Szkurlat A (2001) Electrochim Acta 46:4007
21. Brumbach M, Veneman PA, Marrikar FS, Schulmeyer T, Simmonds A, Xia W, Lee P, Armstrong NR (2007) Langmuir 23:11089
22. Gunawardena GA, Hills G, Montenegro I, Scharifker B (1982) J Electroanal Chem 138:225
23. Kim JY, Kim SH, Lee HH, Lee KH, Ma WL, Gong X, Heeger AJ (2006) Adv Mater 18:572
24. Duren JKJ, Loos J, Morrisey F, Leewis CM, Kivits KPH, IJzendoorn LJ, Rispens MT, Hummelen JC, Janssen RAJ (2002) Adv Funct Mater 12:665
25. Schroder DK (2006) Semiconductor Material and Device Characterization. John Wiley & Sons Inc, New Jersey
26. Valaski R, Roman LS, Micaroni L, Hümmelgen IA (2003) Eur Phys J E 12:507
27. Harris D, Dorsinville R, Mukai T (1997) Appl Phys Lett 70:1216